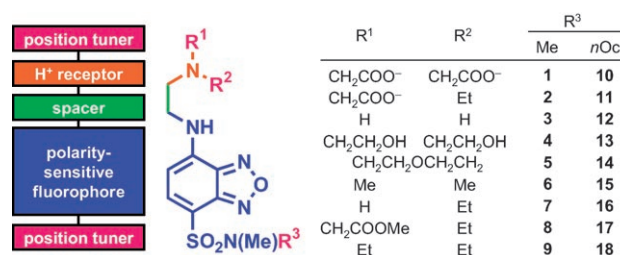


Multiplexing Sensory Molecules Map Protons Near Micellar Membranes**

Seiichi Uchiyama,* Kaoru Iwai, and A. Prasanna de Silva*

Fluorescent sensors^[1] have great potential to operate as molecular-level devices^[2] in nanospaces. Generally, a fluorescent sensor monitors a single parameter of its local environment, such as ion concentration. More functionalized systems which operate according to similar principles are molecular logic gates.^[3] These gates respond to multiple parameters simultaneously according to defined Boolean transformations. There are also a few examples of molecular sensors which respond to multiple parameters, each by a different analytical technique.^[4] Herein we demonstrate a new multiplexing fluorescent sensor which simultaneously monitors multiple parameters (local proton concentration and polarity in this instance) by multiple emission properties (intensity and wavelength, respectively).^[5] As the polarity of spherical micelles in water is expected to change largely monotonically along a radial coordinate,^[6] polarity data translate into positions. We can thus obtain local proton densities at various positions by scattering a series of multiplexing sensors widely over the aqueous micellar field. Therefore a nanoscaled mapping of proton concentration emerges for this simple membrane system. Proton concentration gradients are responsible for the subject of bioenergetics.^[7] Multiplexing sensors also correspond to nanoscale versions of robotic vehicles which go to humanly inaccessible spaces, map local properties and send information back to us.

Scheme 1 shows the structures of the fluorescent multiplexing sensors **1–18** used in this study. These sensors consist of a polarity-sensitive fluorophore (blue), a proton receptor (orange), position tuners (red), and a spacer (green). The sensors function as follows: 1) The local proton concentration



Scheme 1. Fluorescent multiplexing sensors **1–18**. The orders of **1–9** and **10–18** are determined by the log *P* (*n*-octanol/water partition coefficient) value of a corresponding amine R¹R²NH (see the Supporting Information).

is examined by a ΔpK_a value (pK_a in micellar solution – pK_a in water) of a conjugate acid of the receptor amine. This ΔpK_a value is affected by electrostatic potential and dielectric constant at the sensor location but is independent of intrinsic acidity/basicity of the sensor.^[8] If local effective proton concentration is higher than that of bulk water, a positive ΔpK_a value is obtained.^[9] As our sensors possess a fluorescence “off-on” switching system by controlling photoinduced electron transfer processes with a fluorophore–spacer–receptor format,^[1a] the ΔpK_a values can be determined from fluorescence intensity, with pH profiles arising from titrations. 2) The local polarity is estimated from the emission wavelength of the polarity-sensitive fluorophore, 4-sulfamoyl-7-aminobenzofurazan, as its emission wavelength is strongly red-shifted with increasing environmental polarity and is smoothly related to the dielectric constant ϵ of the solvent.^[10] Thus, the relationship between the emission wavelength and the ϵ value is obtained beforehand for each sensor from the fluorescence spectra in water, methanol, and so on (see the Supporting Information). 3) The position of a sensor near micellar membranes is altered by changing its substituents R¹–R³. The sensor bearing more hydrophilic substituents is expected to stay at a more hydrophilic region in the nanospace.^[9a,11] Finally, by collecting the environmental data for **1–18**, proton concentration maps near micellar membranes can be established in the form of ΔpK_a – ϵ diagrams. In the present study, Triton X-100 (neutral, radius: < 4.8 nm^[12]), octyl β -D-glucopyranoside (OG; neutral, ~2.3 nm^[13]), sodium dodecylsulfate (SDS; anionic, < 3.6 nm^[14]), and cetyltrimethylammonium chloride (CTAC; cationic, < 3.5 nm^[14]) are used as micelle media in which the nanoscaled proton gradients are evaluated.

The fluorescence properties of **9** in water and **18** in Triton X-100 aqueous solution during titrations are shown in Figure 1 as representatives of sensory functions. Regarding proton concentration, the ΔpK_a value for **18** in the Triton X-

[*] Dr. S. Uchiyama, Prof. Dr. A. P. de Silva
School of Chemistry and Chemical Engineering
Queen's University, Belfast BT9 5AG (Northern Ireland)
Fax: (+44) 28-9097-4687
E-mail: a.desilva@qub.ac.uk

Dr. S. Uchiyama
Graduate School of Pharmaceutical Sciences
The University of Tokyo
7-3-1 Hongo, Bunkyo-ku, Tokyo 113-0033 (Japan)
Fax: (+81) 3-5841-4768
E-mail: seiichi@mol.f.u-tokyo.ac.jp

Prof. Dr. K. Iwai
Department of Chemistry, Faculty of Science
Nara Women's University
Kitaouya-Nishimachi, Nara 630-8506 (Japan)

[**] We thank The Daiwa Anglo-Japanese Foundation, Invest NI (RTD COE 40) (Japan) Society for the promotion of Science, W. T. Silva and S. T. Herath for support and help.

Supporting information for this article is available on the WWW under <http://dx.doi.org/10.1002/anie.200801516>.

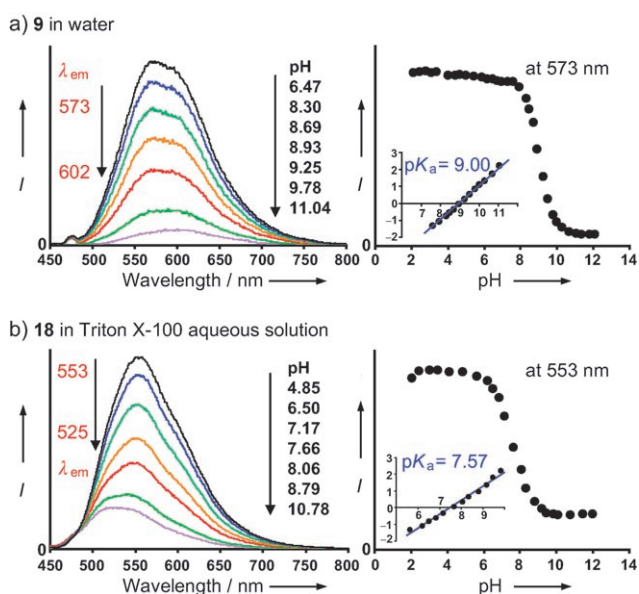


Figure 1. Fluorescence behavior of a) **9** in water and b) **18** in Triton X-100 solution with varying bulk pH. Left: spectra, right: intensities, where I is the fluorescence intensity. Vertical axes for the insets: $\log[(I_{\max}-I)/(I-I_{\min})]$. Excitation wavelength was 410 nm, and concentrations were 10 μM for **9** and **18** and 0.52 mM for Triton X-100.

100 solution is obtained in a straightforward manner from the two pK_a values as -1.43 ($7.57-9.00$).^[15] In contrast, the estimation of local dielectric constants from the emission wavelengths required a longer procedure because of the difference in polarity sensing properties between acidic and basic conditions. The emission wavelengths of **1-18** are blue-shifted by protonation of the amine receptor in homogeneous medium. For example, the emission wavelength of **9** in acidic water is 573 nm, whereas that in basic water is 602 nm (Figure 1 a). This shift is due to an interaction between the protonated receptor and the internal charge transfer excited state of the fluorophore across the dimethylene spacer.^[16] Thus, two relationships (i.e., acidic and basic versions) between the emission wavelength and the ϵ value of solvent are needed for the estimation of local polarity near sensors. For the case of **18** in Triton X-100 aqueous solution (Figure 1 b), the local ϵ values are estimated to be 34 and 2 in the acidic and basic conditions, respectively, from the emission wavelengths (553 and 525 nm; see the Supporting Information).^[17] An important phenomenon which emerged from the collected ϵ values is that the sensor changed its position near the micellar membrane as the conditions changed from acidic to basic. As the protonation of the receptor increases its hydrophilicity, the sensor in acidic condition was located at a more hydrophilic region of the micelle.

Figure 2 shows the $\Delta pK_a-\bar{\epsilon}$ diagrams for the four kinds of micelles. As mentioned above, the positions of the sensors varied between acidic and basic conditions. Taking this fact into the consideration, the median $\bar{\epsilon}$ value ($\bar{\epsilon}$) is adopted as a parameter of polarity near a sensor.^[18] Figure 2 a is the $\Delta pK_a-\bar{\epsilon}$ diagram of Triton X-100. As expected, the sensors are distributed at different positions, from bulk water (equivalent to $\bar{\epsilon}=78.5$) to the micellar interior ($\bar{\epsilon}=18$). The more

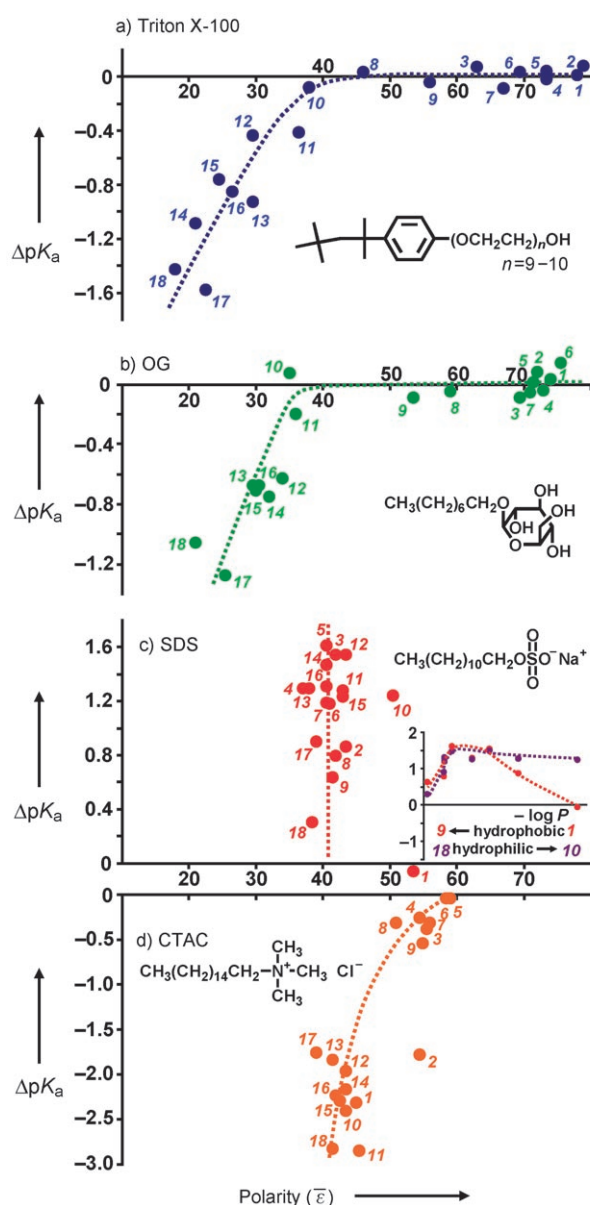


Figure 2. ΔpK_a -polarity ($\bar{\epsilon}$) diagrams obtained for **1-18** (10 μM). a) Triton X-100 (0.52 mM), b) OG (34 mM), c) SDS (0.20M), and d) CTAC (5.0 mM). The numbers in italics represent the sensor corresponding to each point. Dotted lines indicate trends in points.

hydrophobic series (**10-18**) stayed at more hydrophobic regions (lower $\bar{\epsilon}$ values). In Figure 2 a, the ΔpK_a value gradually decreases when the polarity decreases, i.e., as the sensor goes towards the micellar interior.^[6] In particular, **18** gave $\Delta pK_a = -1.43$, meaning that available protons near **18** are only 3.7% of that in bulk water. This negative ΔpK_a value can be attributed to the dielectric effect of the micelle,^[8a] which is unfavorable for protonated amine receptors. Our sensors successfully plot the nanoscaled gradual decrease in the effective proton concentration near the Triton X-100 micelle as moving from bulk water towards the micelle core.

Figure 2 b shows the $\Delta pK_a-\bar{\epsilon}$ diagram for another neutral micelle, OG. Compared to that for Triton X-100, several sensors (**1-7** or **12-16**) gathered around a narrow range of polarity. Nevertheless, a similar $\Delta pK_a-\bar{\epsilon}$ pattern is seen, which

suggests that the dielectric effect on the local proton concentration is independent of the chemical structure of non-ionic membranes (Figure 2).

The $\Delta pK_a-\bar{\epsilon}$ diagram for an anionic SDS micelle is indicated in Figure 2c. Unexpectedly, the sensors show a very narrow range of polarity ($37 < \bar{\epsilon} < 44$), with the exception of **1** and **10**. This means that the fluorophores are evidently pinned at one place, regardless of the R¹–R³ groups. This positional pinning is probably due to the strong ion–dipole interaction between the anionic head groups of the SDS micelles and the fluorophore with the large dipole moment ($\mu = \approx 6.4$ D).^[19] In contrast, the receptor moieties of **1–18** changed their positions because the flexibility of the dimethylene spacer allowed these positional variations. The inset in Figure 2c shows the relationship between the ΔpK_a value and the hydrophobicity of the R¹ and R² groups. In the series of **1–9** (red line), the positive ΔpK_a value is found as the hydrophobicity increased, starting from the case of **1**. As SDS has an anionic head group, protons are concentrated near the surface of the micelles by the electric effect.^[8a,9a] For instance, the free proton concentration near **5** increases by 1.61 pK_a units (= 4070% of that in bulk water). In the **10–18** series (purple), even the most hydrophilic **10** is located near the head groups of the SDS micelles to give a positive ΔpK_a value. In both series, the most hydrophobic **9** and **18** sensed the negative dielectric effect in addition to the positive electric effect, which is why their ΔpK_a values are close to zero.

Figure 2d shows the map for cationic CTAC micelles, where the ion–ion attraction exists between the cationic head group of CTAC and **1**, **2**, **10**, and **11** bearing one or two anionic carboxylate group(s). In addition, the ion–dipole interaction can be anticipated between the cationic head groups and the fluorophore. However, some positional variation, especially owing to the R³ group, is observed ($39 < \bar{\epsilon} < 59$). In the CTAC micelles, both the dielectric and electric effects cooperatively decrease the ΔpK_a value. Therefore a large negative ΔpK_a value (–2.83) is seen for **18** and protons are much less available at the location of **18** (0.15% of bulk water).

In conclusion, the proton concentration maps near the Triton X-100, OG, SDS, and CTAC micelles are obtained by the fluorescent multiplexing sensors **1–18**. These sensors can change their positions and report the multiple information comprised of pK_a values and emission wavelengths. As the entire radial distances of the micelles investigated are less than 5 nm, the space resolution opened up by the present technique is remarkably high. This approach can be easily applied to similar environmental mapping within other nanospaces and of other chemical species. The charged head groups of SDS and CTAC interfered with the positional change of the sensors. Overcoming this interaction will be among further developments of nanoscaled environmental mapping with fluorescent multiplexing sensors.

Received: March 31, 2008

Published online: May 21, 2008

Keywords: fluorescence spectroscopy · fluorescent probes · micelles · molecular devices · sensors

- [1] a) A. P. de Silva, H. Q. N. Gunaratne, T. Gunnlaugsson, A. J. M. Huxley, C. P. McCoy, J. T. Rademacher, T. E. Rice, *Chem. Rev.* **1997**, *97*, 1515–1566; b) J. F. Callan, A. P. de Silva, D. C. Magri, *Tetrahedron* **2005**, *61*, 8551–8588; c) E. V. Anslyn, *J. Org. Chem.* **2007**, *72*, 687–699.
- [2] a) J.-P. Sauvage, *Acc. Chem. Res.* **1998**, *31*, 611–619; b) C. P. Collier, E. W. Wong, M. Belohradský, F. M. Raymo, J. F. Stoddart, P. J. Kuekes, R. S. Williams, J. R. Heath, *Science* **1999**, *285*, 391–394; c) V. Amendola, L. Fabbrizzi, C. Mangano, P. Pallavicini, *Acc. Chem. Res.* **2001**, *34*, 488–493; d) V. Balzani, A. Credi, M. Venturi, *Molecular Devices and Machines*, Wiley-VCH, Weinheim, **2003**; e) V. Serreli, C.-F. Lee, E. R. Kay, D. A. Leigh, *Nature* **2007**, *445*, 523–527; f) S. Kobatake, S. Takami, H. Muto, T. Ishikawa, M. Irie, *Nature* **2007**, *446*, 778–781.
- [3] a) A. P. de Silva, H. Q. N. Gunaratne, C. P. McCoy, *Nature* **1993**, *364*, 42–44; b) A. P. de Silva, N. D. McClenaghan, *Chem. Eur. J.* **2004**, *10*, 574–586; c) S. Uchiyama, N. Kawai, A. P. de Silva, K. Iwai, *J. Am. Chem. Soc.* **2004**, *126*, 3032–3033; d) U. Pischel, *Angew. Chem.* **2007**, *119*, 4100–4115; *Angew. Chem. Int. Ed.* **2007**, *46*, 4026–4040; e) A. P. de Silva, S. Uchiyama, *Nat. Nanotechnol.* **2007**, *2*, 399–410.
- [4] a) M. Schmittel, H.-W. Lin, *Angew. Chem.* **2007**, *119*, 911–914; *Angew. Chem. Int. Ed.* **2007**, *46*, 893–896; b) T. Suzuki, K. Ohta, T. Nehira, H. Higuchi, E. Ohta, H. Kawai, K. Fujiwara, *Tetrahedron Lett.* **2008**, *49*, 772–776.
- [5] For related but different ideas, see: a) M. D. P. de Costa, A. P. de Silva, S. T. Pathirana, *Can. J. Chem.* **1987**, *65*, 1416–1419; b) K. R. A. S. Sandanayake, T. D. James, S. Shinkai, *Chem. Lett.* **1995**, 503–504.
- [6] J. H. Fendler, *Membrane Mimetic Chemistry*, Wiley, New York, **1983**, pp. 6–47.
- [7] F. M. Harold, *The Vital Force—A Study of Bioenergetics*, Freeman, New York, **1986**.
- [8] a) M. S. Fernández, P. Fromherz, *J. Phys. Chem.* **1977**, *81*, 1755–1761; b) C. J. Drummond, F. Grieser, T. W. Healy, *J. Phys. Chem.* **1988**, *92*, 2604–2613; c) T. Pal, N. R. Jana, *Langmuir* **1996**, *12*, 3114–3121.
- [9] a) R. A. Bissell, A. J. Bryan, A. P. de Silva, C. P. McCoy, *J. Chem. Soc. Chem. Commun.* **1994**, 405–407; b) Y. Singh, A. Gulyani, S. Bhattacharya, *FEBS Lett.* **2003**, *541*, 132–136.
- [10] S. Uchiyama, Y. Matsumura, A. P. de Silva, K. Iwai, *Anal. Chem.* **2003**, *75*, 5926–5935.
- [11] a) E. Bardez, E. Monnier, B. Valeur, *J. Phys. Chem.* **1985**, *89*, 5031–5036; b) E. C. C. Melo, S. M. B. Costa, A. L. Maçanita, H. Santos, *J. Colloid Interface Sci.* **1991**, *141*, 439–453; c) W. H. Steel, R. A. Walker, *Nature* **2003**, *424*, 296–299.
- [12] P. S. Goyal, S. V. G. Menon, B. A. Dasannacharya, P. Thiyagarajan, *Phys. Rev. E* **1995**, *51*, 2308–2315.
- [13] B. Lorber, J. B. Bishop, L. J. DeLucas, *Biochim. Biophys. Acta Biomembr.* **1990**, *1023*, 254–265.
- [14] V. K. Aswal, P. S. Goyal, *Phys. Rev. E* **2000**, *61*, 2947–2953.
- [15] The ΔpK_a values for **10–18** are determined by using the pK_a values for **1–9** in water instead of those for **10–18** because of insolubility.
- [16] A. P. de Silva, H. Q. N. Gunaratne, J.-L. Habib-Jiwan, C. P. McCoy, T. E. Rice, J.-P. Soumillion, *Angew. Chem.* **1995**, *107*, 1889–1891; *Angew. Chem. Int. Ed. Engl.* **1995**, *34*, 1728–1731.
- [17] In the linear relationships between the emission wavelength and the ϵ value of solvent, **1–9** are treated as model compounds of **10–18**, as **10–18** are insoluble in water.
- [18] The use of differently weighted averages of two ϵ values did not affect the relative pattern of ΔpK_a –polarity diagrams.
- [19] S. Uchiyama, T. Santa, K. Imai, *J. Chem. Soc. Perkin Trans. 2* **1999**, 569–576.